A probabilistic fracture mechanics method and strength analysis of glulam beams with holes

Henrik Danielsson, Per Johan Gustafsson

A Probabilistic Fracture Mechanics Method and Strength Analysis of Glulam Beams with Holes

Henrik Danielsson* & Per Johan Gustafsson
Division of Structural Mechanics, Lund University, Sweden
P.O. Box 118, SE-221 00, Lund, Sweden
** corresponding author:* henrik.danielsson@construction.lth.se

Abstract

A probabilistic fracture mechanics method is presented and applied to glulam beams with holes. The method is based on a combination of Weibull weakest link theory and a mean stress method which is a generalization of linear elastic fracture mechanics. Combining these two methods means that the global strength will be governed by both fracture energy and material strength and also that the stochastic nature of the material properties are taken into account. The probabilistic fracture mechanics method is evaluated by comparison to experimental test results. The method shows good ability to predict strength, with the exception of very small beams where the capacity is overestimated. The comparison to experimental tests deals also with other methods for strength analysis including code design methods.

Probabilistische Bruchmechanik und Festigkeitsanalyse von Brettschichtholzträgern mit Durchbrüchen

Zusammenfassung

Ein probabilistisches Bruchmechanikverfahren wird vorgestellt und auf Brettschichtholzträgern mit Durchbrüchen angewandt. Grundlage dieser Methode ist eine Kombination der Weibull Theorie des schwächsten Gliedes und der Methode der mittleren Spannung, einer Verallgemeinerung der linear-elastischen Bruchmechanik. Die Kombination dieser beiden Methoden bedeutet, dass die globale Festigkeit sowohl von der Bruchenergie als auch der Materialfestigkeit bestimmt wird und dass die stochastische Natur der Materialeigenschaften berücksichtigt wird. Das probabilistische Bruchmechanikverfahren wird durch Vergleich mit Versuchsergebnissen überprüft. Das Verfahren erweist sich als gut geeignet zur Vorhersage der Festigkeit mit Ausnahme von sehr kleinen Trägern, deren Tragfähigkeit überschätzt wird. Mit den Versuchsergebnissen werden auch andere Methoden der Festigkeitsanalyse einschließlich normierter Bemessungsverfahren verglichen.

1 Introduction

Introducing a hole through a glulam beam drastically changes the stress state and reduces the strength significantly due to the high perpendicular to grain tensile stresses and the shear stresses appearing in the vicinity of the hole. It is however sometimes necessary to make a hole, for example for installations such as ventilation pipes. Wood is weak when loaded in tension perpendicular to grain and fracture caused by this type of loading commonly has a brittle course, which emphasizes the need for careful design.

Finding a simple, general and reliable design method is however a difficult task. Looking at European timber engineering design codes over the last decades, it can be seen that strength design of glulam beams with holes have been treated in many different ways. The theoretical backgrounds on which the recommendations are based show fundamental differences and there are also major discrepancies between strength predictions according to different codes as well as between codes and experimental tests (Aicher and Höfflin 2004; Danielsson 2007; Danielsson and Gustafsson 2008). The lack of knowledge is further reflected by the fact that the contemporary version of the European timber code Eurocode 5 (SS-EN 1995-1-1 2004) does not state any equation concerning design of beams with holes. The recommendations in the German timber code DIN 1052:2004-08 were further withdrawn for circular and rectangular holes during 2007, reportedly this was because of general safety and reliability concerns. The new German code DIN 1052:2008-12 however contains modified design recommendations accounting also for a beam height effect which was not accounted for in the previous version of the code.

The hypothesis in this study is that accurate strength predictions for glulam beams with holes can be obtained by what can be referred to as a *probabilistic fracture mechanics method*. A proposal for such a method is briefly outlined in Gustafsson and Serrano (1999) and will be further developed here. The considered method is based on a combination of Weibull weakest link theory and a mean stress method which is a generalization of linear elastic fracture mechanics. Combining these two methods means that the global strength will be governed by both fracture energy and material strength and also that the stochastic nature of the material properties are taken into account. The method is derived within the framework of continuum mechanics of a stochastically homogeneous orthotropic material and applied to strength analysis of glulam beams with holes considering two-dimensional plane stress conditions.

The aim of the study is to investigate the possibilities of the proposed method. Specifically, the influence of four important design parameters on the strength is considered for both quadratic and circular holes: bending moment to shear force ratio, beam size, hole placement with respect to beam height and relative hole size with respect to beam height. Strength predictions according to the probabilistic fracture mechanics method are also compared to experimental test results and other methods for strength analysis including code design methods.

The strength considered in this paper is the short term static strength. The presented strength analysis method is based on strength limitation due to fracture along grain, caused by combined action of perpendicular to grain tensile stress and shear stress, which is believed to be the most relevant failure mechanism for glulam beams with holes. Hence, other failure modes such as finger joint failures and bending failures due to parallel to grain tensile or compressive stress are not considered. Issues relating to long term loading, cyclic fatigue, moisture variation and transverse stability are, although they may be of importance in practical design, out of scope in the present study. These issues are in timber engineering design codes commonly dealt with by separate considerations.

2 Methods for rational strength analysis

There are a few basically different methods for rational strength analysis based on linear elastic stress analysis within the framework of continuum mechanics. The first difference considered here relates to whether material strength properties are assumed to be homogeneous or heterogeneous and hence to whether a deterministic or a stochastic approach is used. The second difference considered here relates to whether an ideally brittle material behavior is assumed or not. In this context, an ideally brittle

material refers to a material for which the fracture process region at the instant of start of crack propagation is very small (infinitesimally small), even approaching zero. The size of the fracture process region is related to, and commonly proportional to, the material property ratio EG_c/f^2 where E is a measure of stiffness, G_c a measure of the fracture energy and f a measure of the strength of the material. By this definition, a fracture process region of zero size and hence an ideally brittle material is obtained for zero fracture energy or for infinite material strength.

The dominating method in timber engineering is what can be referred to as *conventional stress analysis* (here abbreviated CSA) based on assumptions of a homogeneous, ideally brittle material and with some stress based failure criterion. Hence, the global strength is reached when the stress equals the material strength in the most stressed point. The fracture energy is not explicitly included in CSA but assuming fracture at the instant the failure criterion is fulfilled, zero fracture energy is implicitly assumed. This type of strength analysis method is of little use for glulam beams with a hole due to the high stress gradients in the vicinity of the hole.

The *Weibull weakest link theory* (Weibull 1939) is, just as CSA, based on the assumptions of an ideally brittle material but the material strength properties are however allowed to be heterogeneous. Weibull theory has been applied to glulam beams with circular holes, showing no stress singularity (Aicher and Höfflin 2004; Höfflin 2005; Aicher et al. 2007). A general drawback of Weibull theory and CSA is however that they cannot be applied to strength analysis of structural elements with a stress singularity caused by a crack or a sharp notch (Gustafsson and Enquist 1988).

Also in *linear elastic fracture mechanics* (LEFM), an ideally brittle material is considered. The material strength is implicitly assumed to be infinite and the global strength is instead governed by fracture energy properties. Application of LEFM to timber/glulam beams with holes in particular is presented in e.g. Pizio (1991), Aicher et al. (1995), Peterson (1995), Riipola (1995), Scheer and Haase (2000), and Gustafsson (2002). LEFM suffers however from a major limitation: it is based on the assumption of an existing crack giving rise to a square root stress singularity. The theory can however be modified (generalized) in order to overcome this limitation. The *mean stress method* is one such generalization. Since the fracture process region in any real material is nonzero due to nonzero fracture energy and finite material strength, the basic idea of this method is to consider the mean tensile and shear stresses acting within a certain area. These stresses, which have a finite value also for the case of presence of a stress singularity, are then used in a conventional stress based failure criterion. This approach enables analysis of bodies with or without a square root stress singularity and the global strength is governed by both fracture energy properties and material strength properties. The mean stress method has been applied to glulam beams with holes (Gustafsson 2002) and has recently also been applied to steel-timber dowel joints (Sjödin and Serrano 2008).

Furthermore, there are numerous methods of varying complexity relating to *nonlinear fracture mechanics*. An application of nonlinear fracture mechanics to glulam beams with holes is found in Schmidt and Kaliske (2009), where a material model including anisotropic multi-surface plasticity for compression and including traction-separation laws for tension and shear is presented. Probabilistic methods, related to the present method in the sense that some statistical approach is used to account for the stochastic nature of variables, have for example also been used for wood applications in relation to LEFM in Foschi et al. (1989), and in relation to damage mechanics analysis of the heterogeneous microstructure of wood in Vasic et al. (2005).

3 A probabilistic fracture mechanics method

The probabilistic fracture mechanics method (here abbreviated PFM) considered here is based on a combination of Weibull theory and a mean stress method. The derivation of PFM starts with considerations according to Weibull theory (Weibull 1939). The basic assumption in Weibull theory is that the behavior of a material volume resembles the behavior of a chain of links coupled in series and loaded in tension: global failure occurs when the strength of the weakest link is reached. The strength of the links are assumed to be statistically equal and described by a failure probability function F, which is a function of stress. There are different suggestions for the function F but within timber engineering, Weibull's two-parameter model is the most frequently used one and the failure probability function F is then given by

$$F = 1 - e^{-\left(\frac{\sigma}{\sigma_0}\right)^m} \tag{1}$$

where σ is the stress, σ_0 is the scale parameter related to the magnitude of material strength and m the Weibull shape parameter related to the scatter in material strength. Considering a volume Ω with an arbitrary stress distribution $\sigma(x,y,z)$, the global failure probability F_{global} is found to be

$$F_{global} = 1 - e^{-\int_\Omega \left(\frac{\sigma(x,y,z)}{\sigma_0}\right)^m} \tag{2}$$

Using Equation (2) for analysis of different volumes and stress distributions with equal global probability of failure, the following expression can be obtained (Danielsson 2009)

$$\frac{\sigma_{max}}{f} = \left(\frac{1}{\Omega_{ref}}\int_\Omega \left(\frac{\sigma(x,y,z)}{f_{ref}}\right)^m d\Omega\right)^{1/m} \tag{3}$$

where σ_{max} for a given magnitude of the external load is the maximum stress in the body of volume Ω and with stress distribution $\sigma(x,y,z)$. Due to the scatter in strength is σ_{max} at the instant of failure different for different nominally equal bodies. f is the mean of the failure value of σ_{max} and f_{ref} is the mean strength valid for a homogeneous stress distribution in the reference volume Ω_{ref}.

The ratio σ_{max}/f can be interpreted as a global effective dimensionless stress parameter α_{global} and $\sigma(x,y,z)/f_{ref}$ as an effective dimensionless stress field $\alpha(x,y,z)$ defined in the volume Ω. The expression can then be rewritten as

$$\alpha_{global} = \left(\frac{1}{\Omega_{ref}}\int_\Omega \alpha^m(x,y,z)\, d\Omega\right)^{1/m} \tag{4}$$

where the value of α_{global} for $\alpha(x,y,z)$ in Ω corresponds to equal probability of failure as the constant value of $\alpha(x,y,z)=\alpha_{global}$ for a homogeneous stress in Ω_{ref}. Since f_{ref} is here defined as the mean strength of Ω_{ref}, $\alpha_{global}=1.0$ will for Ω give the mean failure value of σ_{max}. The magnitude of the stress $\sigma(x,y,z)$ and thus also $\alpha(x,y,z)$ and α_{global} are for linear elastic materials proportional to the external load. This facilitates calculation of the external load that gives $\alpha_{global}=1.0$.

The effective dimensionless stress field $\alpha(x,y,z)$ is not limited to being based on a single stress component and its corresponding strength value but may very well be expressed as an effective stress based on two or several stress components. For the present application with crack propagation along grain due to perpendicular to grain tensile stress combined with shear stress, it is reasonable to

disregard possible influence of normal stress along grain and then define the effective dimensionless stress field according to the Norris failure criterion (Norris 1962)

$$a(x,y,z) = \left(\left(\frac{\sigma(x,y,z)}{f_\sigma} \right)^2 + \left(\frac{\tau(x,y,z)}{f_\tau} \right)^2 \right)^{1/2} \quad (5)$$

where $\sigma(x,y,z)$ and $\tau(x,y,z)$ are the perpendicular to grain tensile stress and the shear stress and f_σ and f_τ are the corresponding mean strengths valid for the reference volume Ω_{ref}.

Acknowledging the heterogeneity in material strength in this way, the global strength will be governed by the magnitude and the scatter in material strength and will further be influenced by both the stressed volume and the stress distribution. As mentioned above, unrealistic strength predictions will however be obtained for bodies with a stress singularity caused by a crack or a sharp notch (Gustafsson and Enquist 1988). To overcome this limitation and to account also for a nonzero size of the fracture process region due to nonzero fracture energy, another choice of the effective dimensionless stress field can be made. The particular choice made here is based on considerations according to a mean stress method. The stresses σ and τ are in Equation (5) replaced by the corresponding mean stresses $\bar{\sigma}$ and $\bar{\tau}$ which are the mean stresses within what is referred to as a *potential fracture area*. For plane stress conditions, the effective dimensionless stress field can then be expressed as

$$a(x,y) = \left(\left(\frac{\bar{\sigma}(x,y)}{f_\sigma} \right)^2 + \left(\frac{\bar{\tau}(x,y)}{f_\tau} \right)^2 \right)^{1/2} \quad (6)$$

where if the mean stress perpendicular to grain is compressive, this contribution is ignored and the effective dimensionless stress is determined by the mean shear stress only.

The size of the potential fracture area is related to the size of the fracture process zone at the instant of start of crack growth and defined by the plane stress width and a length in the grain direction. The length of the potential fracture area is derived in such a way that the mean stress method will give the same strength prediction for a body in a homogeneous state of stress as CSA and give the same strength prediction as LEFM for a large body with a square root stress singularity. It is here assumed that this length is the same also for all intermediate stress gradients between the zero stress gradient and the square root stress singularity gradient. For a potential fracture area starting from a surface of the body, this length is found to be (Gustafsson 2002)

$$a_{mac} = \frac{2}{\pi} \frac{E_I G_{Ic}}{f_\sigma^2} \frac{E_x}{E_y} \left(\frac{G_{IIc}}{G_{Ic}} \right)^2 \frac{1}{4k^4} \left(\sqrt{1 + 4k^2 \sqrt{\frac{E_y}{E_x} \frac{G_{Ic}}{G_{IIc}}}} - 1 \right)^2 \left(1 + k^2 \frac{f_\sigma^2}{f_\tau^2} \right) \quad (7)$$

where $E_I = \sqrt{\frac{2E_x E_y}{\sqrt{\frac{E_x}{E_y}} + \frac{E_x}{2G_{xy}} - \nu_{yx}\frac{E_x}{E_y}}}$

where E_x, E_y, G_{xy} and ν_{yx} are the elastic stiffness parameters (Poisson's ratio defined as $\nu_{yx}=\varepsilon_x/\varepsilon_y$ for uniaxial loading in the y-direction), G_{Ic} and G_{IIc} are the mode I and mode II critical energy release rates (which are equal to the fracture energies for an ideally linear elastic material) and $k = \bar{\tau}(x,y)/\bar{\sigma}(x,y)$ is the mixed mode ratio. The grain direction is here represented by the x-direction.

The expression in Equation (7) is valid for a potential fracture area starting from the surface of the considered body, which corresponds to initiation of fracture at a surface defect. The integration of $\alpha(x,y)$ should however be carried out over the entire considered volume meaning that also interior points need to be considered. The length of the potential fracture area related to an arbitrary material point is denoted a_m and governed by the length a_{ms} stated in Equation (7) and also by the distance x_d from the closest surface to the fracture initiation point in the grain direction. For an interior point at a distance x_d equal to or greater than a_{ms} from a surface, a defect in the material can be interpreted as an interior crack which has two tips and the length of the potential fracture area is hence twice that valid for a surface crack, $a_m=2a_{ms}$. For points which are not on a surface, but neither far from them, some approximation needs to be made. Various methods for this approximation or interpolation are feasible. The method of approximation used in the present calculations is illustrated in Figure 1 and can be expressed mathematically as

$$a_m = \begin{cases} a_{ms} & \text{for} \quad 0 \le x_d < a_{ms}/2 \\ 2x_d & \text{for} \quad a_{ms}/2 \le x_d < a_{ms} \\ 2a_{ms} & \text{for} \quad a_{ms} \le x_d \end{cases} \tag{8}$$

The physical interpretation of the method is that all points in the body are considered as potentially weak points where fracture initiation may occur. The material is, due to fracture toughness and ductility, assumed to have the ability to distribute the stresses over the fracture area and it is hence the mean stresses acting within this area that are considered. In accordance with Weibull theory, the resistance to fracture is not homogeneous but viewed as a stochastic property. The strength prediction according to PFM relates to the instant of start of crack propagation but does however not give any indication on whether the propagation is stable or unstable.

The strength prediction of PFM depends, among other parameters, on the value of the Weibull shape parameter m and the fracture energy parameters G_{Ic} and G_{IIc}. For $G_{Ic}=G_{IIc}=0$, the method will break down to Weibull theory. PFM will also approach Weibull theory for increasing size of the considered body since the relative size of the potential fracture area decreases. For $G_{Ic}\neq 0$, $G_{IIc}\neq 0$ and $m\rightarrow\infty$, PFM will break down to the mean stress method meaning that the potential fracture area with the most severe combined action of $\bar{\sigma}$ and $\bar{\tau}$ will be decisive. For the special case of a deep crack in a large body, the mean stress method will in turn break down to conventional LEFM. For $G_{Ic}=G_{IIc}=0$ and $m\rightarrow\infty$, the strength prediction of PFM will be the same as according to CSA and the material point with the most severe combined action of σ and τ will be decisive.

4 Method for strength analysis of glulam beams with holes by probabilistic fracture mechanics

4.1 Determination of stress fields

The stress fields $\sigma(x,y)$ and $\tau(x,y)$ are determined by 2D plane stress finite element analysis by the commercial software Abaqus. The entire beam is not modeled but only a certain part of the beam close to the hole according to Figure 2. The reason for adopting this approach is that it decreases the computational demands and enables an easy way of changing load conditions. The geometry is defined by the beam height H, beam width T, hole side lengths a and b, hole corner radius r and position of hole center relative to the neutral axis of the beam s. A circular hole can formally be regarded as a quadratic hole with diameter $\Phi=a=b=2r$. The length of the beam part considered for the

finite element stress analysis is $1.5H$+$1.5H$. The shear forces V and the bending moments M_L and M_R are applied as parabolic shear stress distributions and linear normal stress distributions respectively. The load condition is represented by the bending moment to shear force ratio $M/(VH)$ at hole center.

An orthotropic and linear elastic material model is used with stiffness properties according to Table 1. 8-node plane stress quadrilateral elements with biquadratic displacement interpolation and reduced integration are used. Dynamic and geometrical non-linear effects are not included in the analysis. A typical finite element mesh used for the stress analysis is shown in Figure 3.

4.2 Determination of mean stresses

The output from the finite element stress analysis is taken as the stresses σ and τ in the nodal points of the elements. These stresses are then interpolated at reference points in an evenly distributed grid in the body. The distance between the reference points is equal in x- and y-directions and is denoted a_{rp}. For the presented numerical calculations is $a_{rp}=H/1000$. The mean stresses $\bar{\sigma}(x,y)$ and $\bar{\tau}(x,y)$ are determined at all reference points by numerical integration of the stresses within the potential fracture area a_m associated with the specific reference point. The size of the potential fracture area depends on the mixed mode ratio $k = \bar{\tau}(x,y)/\bar{\sigma}(x,y)$ and determining the mean stresses is hence an iterative process. In this implementation, this iteration is however ignored and the mixed mode ratio is assumed to be determined with sufficient accuracy by the ratio between the stresses in the considered reference point $k = \tau_i/\sigma$.

The mean stresses must be determined in a part of the beam somewhat smaller than the one used for the finite element stress analysis. The reason for this is that the mean stresses in an interior material point of the body represent stress of both sides of the material point in the x-direction. The mean stresses are for the presented numerical calculations determined within a length $0.75H$+$0.75H$. Increasing this length has only a very small influence on strength prediction since the perpendicular to grain tensile stress which gives the dominating contribution to α_{global} is limited to the close vicinity of the hole (Danielsson 2009).

4.3 Stress integration and strength prediction

The strength prediction according to the probabilistic fracture mechanics method is implicitly given by the value of the global effective dimensionless stress parameter α_{global} which is determined by integration of the effective dimensionless stress field $\alpha(x,y)$ according to Equation (4). This integration is carried out numerically according to

$$\alpha_{global} = \left(\frac{A_{ref}}{\Omega_{ref}} \sum_{i=1}^{n} \alpha^m(x_i,y_i) \right)^{1/m} \quad (9)$$

where n is the number of reference points in the body and $\alpha(x_i,y_i)$ is the effective dimensionless stress at reference point i according to Equation (6). The criterion $\alpha_{global}=1.0$ gives the mean global failure load since α_{global} is proportional to the applied loads and the strength prediction in terms of shear force at failure $V_{failure}$ is hence given by

$$V_{failure} = \frac{1}{\alpha_{global}} V_{FE} \quad (10)$$

where V_{FE} is the shear force applied in the finite element stress analysis and α_{global} is the value obtained from Equation (9) for this applied shear force.

Illustrations of typical distributions of σ, τ, α and α^m in the vicinity of a hole are shown in Figure 4. It is from the distribution of α^m evident that the two regions that contribute significantly to α_{global} are very small. The illustration is based on the material properties stated in Table 1. Beam geometry and load condition are H=600 mm, T=115 mm, a=b=0.30H, r/a=r/b≈0.14, s=0, M/(VH)=4.0 and the applied load corresponds to the PFM failure load $V_{failure}$=56 kN.

4.4 Material properties

The material properties used for the numerical calculations are given in Table 1. The stiffness properties E_{xx}, E_{yy}, G_{xy} and ν_{yx} are assumed to correspond to mean values valid for glulam strength class GL 32h. The material strengths f_σ and f_τ and the fracture energies G_{Ic} and G_{IIc} are also assumed to correspond to mean values and are based on values used in Gustafsson (2002). The values of the reference volume Ω_{ref} and the Weibull shape parameter m relate to experimental tests of the strength for homogeneous tensile stress perpendicular to grain. The reference volume Ω_{ref} is determined from the empirical relation

$$\frac{f_\sigma}{f_0} = 1.5\left(\frac{\Omega_{ref}}{\Omega_0}\right)^{-0.2} \tag{11}$$

where f_0=1.0 MPa and Ω_0=10^6 mm^3 which is found in Gustafsson (2003). The chosen value of the Weibull shape parameter, m=5, corresponds to the volume influence in the above given equation and also to about 23% coefficient of variation in strength.

5 Verification: Beam in bending

In order to verify the numerical implementation, the method is applied to a beam in bending according to Figure 5. For this loading and geometry, an analytical solution is derived in Danielsson (2009) according to

$$M_{failure} = \frac{TH^2 f_\sigma}{6}\frac{1}{1-a_{ms}/H}\left(\frac{LHT}{2\Omega_{ref}}\left(\frac{a_{ms}}{H}+\frac{1}{m+1}-\frac{1}{m+1}\frac{a_{ms}}{H}\right)\right)^{-1/m} \tag{12}$$

where $a_{ms} = \frac{2E_I G_{Ic}}{\pi f_\sigma^2}$

The results for the special cases of the mean stress method and Weibull theory are found by $m\rightarrow\infty$ and a_{ms}=0 respectively. The strength prediction according to the analytical solutions (dashed and solid lines) and the numerical solutions (marks) are for different values of m and G_{Ic} shown in Figures 6 and 7 for the probabilistic fracture mechanics method (PFM), Weibull theory (WEI), the mean stress method (MSM) and also according to conventional stress analysis (CSA) with failure criterion σ=f_σ. The numerical implementation of PFM gave almost exactly the same results as the analytical solution.

As can be seen in Figure 6, the predicted strength of PFM approaches the one of MSM and the predicted strength of WEI approaches the one of CSA for increasing m. Increasing value of the Weibull parameter m corresponds to decreasing variation in material strength and hence to increasing significance of the most stressed potential fracture area and most stressed point for PFM and WEI respectively. As can be seen in Figure 7, the predicted strength of MSM approaches the one of CSA and the predicted strength of PFM approaches the one of Weibull theory for decreasing fracture energy which corresponds to decrease in length of the potential fracture area.

The verification is based on a beam of dimension L=2H=2T=200 mm. The material properties other than the ones illustrated in these two figures are as stated in Table 1. Applying a pure bending moment gives a mixed mode ratio k=0 and with the given material properties a_{ms}≈21 mm.

6 Parameter study and verification

The parameter study and verification concern the four design parameters bending moment to shear force ratio M/VH, beam size H, hole placement with respect to beam height s/H and relative hole size with respect to beam height a/H=b/H or Φ/H. The applied loads and the geometry parameters are defined in Section 4.1 and Figure 2. The relative influences on the strength of the four design parameters are illustrated in Figure 8 for a beam with a quadratic hole with rounded corners and in Figure 9 for a beam with a circular hole. The illustrations are based on a reference beam according to the figures. For each of the four graphs in the respective figures, one of the design parameters is varied while the others are constant. The beam capacity according to PFM is represented by the nominal shear strength V/A_{net} where V is the shear force at failure given by Equation (10) which refers to start of fracture along grain caused by perpendicular to grain tensile stress and shear stress. A_{net} is the net cross section area at hole center; A_{net}=T(H-b) for quadratic holes and A_{net}=T(H-Φ) for circular holes. The nominal shear strength V/A_{net} is 1.35 MPa for the reference beam with a circular hole (r/Φ=0.5), 1.16 MPa for the reference beam with a quadratic hole and rounded corners (r/a=r/b≈0.14) and 1.14 MPa for a corresponding quadratic hole with sharp corners (r=0).

Verification of PFM is carried out by comparison to experimental test results. Strength tests of beams with quadratic holes with rounded corners were performed at Lund University (Danielsson 2008). The design parameters primarily studied in this test program were: bending moment to shear force ratio, beam size and hole placement with respect to beam height. For beams with circular holes verification is made by means of test results presented in Höfflin (2005) and Aicher and Höfflin (2006). These studies are two of the most recent and most comprehensive test programs on glulam beams with circular holes and the design parameters primarily studied were: bending moment to shear force ratio, beam size and relative hole size with respect to beam height. A comparison concerning these tests is shown in Figure 10 for quadratic holes and in Figure 11 for circular holes. All beams of the presented tests are of material strength class GL 32h. The strengths of the experimental tests refer to the shear force V when there is a crack spreading across the entire beam width at any (or both) of the two beam parts with tensile stress perpendicular to grain in the vicinity of the hole. The crack does however not need to have propagated in an unstable manner in the beam length direction. This load level is considered to be of importance for design and it also corresponds to the PFM failure criterion.

Some comments on the PFM strength predictions and on their correlation to the experimental test results concerning the four design parameters are given below:

Bending moment to shear force ratio

For holes centrically placed with respect to beam height, PFM predicts decreasing strength for increasing bending moment to shear force ratio. The differences in strength for the considered bending moment to shear force ratios are however comparatively small. According to PFM, the influence of bending moment to shear force ratio seems to a large extent to depend on the hole placement with respect to beam height. This is commented below.

Beam size

PFM predicts a strong beam size influence on the strength which was also found in the experimental tests. Among the four design parameters and within the respective limits presented in Figures 8 and 9, the beam size is the most influential. PFM seems to capture the experimentally found beam size effect well for the beams with circular holes and H=450 and 900 mm, see Figure 11. The method further predicts the absolute strength well for beams with quadratic holes and H=630 mm but however considerably overestimates the capacity for beams with quadratic holes and H=180 mm, see Figure 10. Comments regarding this are found in Section 8.

Hole placement with respect to beam height

Concerning hole placement with respect to beam height, the influence on the strength predicted by PFM is rather complex. For the reference beams in Figure 8 and Figure 9 where $M/(VH)$=4, the strength is greater for the centrically placed holes than for the eccentrically placed ones. Further calculations showed that this difference in strength increases with increasing bending moment to shear force ratio (Danielsson 2009). For holes placed in a position where $M/(VH)$=0, the method however predicts greater strength for eccentrically placed holes than for centrically placed ones. PFM predicts higher strength for test series AUh with a hole placed in the upper part of the beam ($s=H/6$, $M/(VH)$=2) than for test series AMh with a centrically placed hole (s=0, $M/(VH)$=2), see Figure 10. The test results however show the opposite relation. The difference in predicted strength is however small. For the small beams in the same figure, both PFM and the test results show lower strength for eccentrically placed holes. The strength reduction predicted by PFM is however somewhat smaller than found in experimental test.

Relative hole size with respect to beam height

PFM predicts decreasing nominal shear strength with increasing relative hole size. In general, the method suggests greater strength for a beam with a circular hole compared to a beam with a quadratic hole for $a=b=\Phi$. The strength reduction for increasing hole size is further greater for the quadratic holes than for the circular holes. Increasing the holes size from $\Phi=a=b=0.20H$ to $0.40H$, the nominal shear strength is reduced by about 25% for the quadratic holes and about 15% for the circular holes. Compared to experimental test results, PFM seems to predict the influence of relative hole size well. As can be seen in Figure 11, the decrease in nominal shear strength seems in general fairly equal for the test results and PFM.

7 Comparison of methods for strength analysis

A comparison of the overall ability to predict strength of different methods is presented in Figure 12, where the ratio between theoretically predicted capacity and capacity found in experimental tests is given. The comparison concerns the test series presented in Figures 10 and 11 and quadratic and circular marks represent test series with quadratic and circular holes, respectively.

The considered methods are: the probabilistic fracture mechanics method (PFM), Weibull theory considering interaction of σ and τ (WEI$\sigma\tau$) and considering only σ (WEIσ), the mean stress method (MSM), conventional stress analysis considering interaction of σ and τ (CSA$\sigma\tau$) and considering only σ (CSAσ). For the comparison with these general methods, the experimental capacities are represented by the mean values of the test series and the theoretical capacities are based on material properties stated in Table 1 which are assumed to be mean values. Some code design methods are also included in the comparison: the empirically based method (method 1) and the "end-notched beam"-analogy method (method 2) in Limträhandbok (Carling 2001), the old German code DIN 1052:2004-08, the

new German code DIN 1052:2008-12 and also the Weibull-based design proposal by Höfflin and Aicher (Höfflin 2005, Aicher and Höfflin 2006). The latter method is presented for circular holes only, but is here used also for quadratic holes assuming a=b=Φ. The "end-notched beam" method is identical to the design method found in a previous preliminary version of Eurocode 5 (prEN 1995-1-1 2002). Two major changes have been introduced in DIN 1052:2008-12 compared to DIN 1052:2004-08; a beam size influence has been introduced and the restrictions on the maximum allowed hole size are more conservative. For comparison with these code design methods, the theoretical capacities are based on characteristic strengths $f_{v,k}$ = 3.8 MPa and $f_{t,90,k}$ = 0.5 MPa (SS-EN 1194 2000) and the experimental capacities are represented by characteristic capacity V_k of the test series according to

$$V_k = \bar{V}(1 - 1.645\ cov) \tag{13}$$

where $\bar{V}$ is the test series mean shear force strength and *cov* is the coefficient of variation. The beams with quadratic holes and circular holes are treated separately, resulting in *cov*=6.31% for the 32 tests of beams with quadratic holes and *cov*=15.3% for the 56 tests of beams with circular holes. More details regarding the determination of the characteristic test capacities are given in Danielsson and Gustafsson (2008).

Among the presented tests, the test series denoted H4 in Figure 11 shows a surprisingly low strength. The mean shear force strength of this test series is lower than the one of test series A2 which has equal loading conditions and beam geometry but with a larger hole. The test series H4 is in Figure 12 represented by a filled mark.

PFM shows good agreement compared to the test results, with the exception of the four test series with small beams and quadratic holes as previously mentioned. The two methods based on Weibull theory (WEIστ and WEIσ) show overall good agreement compared to the test results used in this comparison. It is remarkable that the agreement is also good for quadratic holes having rounded corners with r/a=r/b≈0.12, since Weibull theory predicts an unrealistic zero strength for quadratic holes with sharp corners r=0.

The "end-notched beam"-analogy method (Limträhandbok method 2) shows the most un-conservative strength predictions among the code design methods. It is however interesting that the scatter in ratio between theoretical and experimental strength is fairly low considering the beams with circular and quadratic holes separately. The overall agreement with experimental test could easily be improved by using some general reduction for beams with circular holes.

The scatter in the ratio between the theoretical capacity and experimental capacity is smaller in DIN 1052:2008-12 compared to DIN 1052:2004-08. This is due to addition of a beam height influence in the later version of the code. The maximum hole size is however in DIN 1052:2008-12 limited to b=Φ=0.15H whereas DIN 1052:2004-08 stated the more generous limit b=Φ=0.40H. Accordingly, all test series presented in Figure 12 have larger holes than allowed in DIN 1052:2008-12.

8 Concluding remarks

The probabilistic fracture mechanics method seems to have good ability to predict the strength of glulam beams with holes, with the exception of small beams. An overestimation of about 30% was found for the small beams (H=180 mm) with quadratic holes. One probable explanation is that the size of the potential fracture area a_m, used to determine mean stresses, is too large in relation to the size of the small beams. The size of a fracture process region can, according to fracture mechanics, be

expected to be governed by the properties of the material and to be independent of the size of the structure only as long as the structure is large as compared to the size of the fracture region. Further decrease in structural size implies decreased size of the fracture region. To overcome this problem, some kind of stress gradient related reduction of the length of the potential fracture area can be introduced for small beams.

Good general features of the probabilistic fracture mechanics method are the ability to analyze holes of arbitrary geometry and to consider the material properties that are believed to be the most important ones for strength of glulam beams with a hole: material strength, fracture energy and heterogeneity. Contemporary code design methods are limited to considering material strength and in some cases also heterogeneity, but in all cases the fracture energy is disregarded. Despite general applicability, the method is furthermore simple in the sense that non-linear stress or fracture course analysis is not required. Although simple in this sense, the presented form of the method is hardly suitable as a code design method. One possibility might however be to deduce relations between various design parameters and beam strength from extensive parameter studies based on PFM and then incorporate these relations in a design method suitable for codes.

A more thorough description of the probabilistic fracture mechanics method, a more comprehensive parameter study and a brief review of the code design methods considered here, except DIN 1052:2008-12, is presented in Danielsson (2009).

Acknowledgements

The financial support from *Formas* through grant 24.3/2003-0711 is greatly appreciated. In relation to the experimental tests carried out at Lund University, the financial support through collaboration with Ulf Arne Girhammar at Umeå University within the project *Multi-story timber frame buildings* (The European Union's Structural Funds – Regional Fund: Goal 1) is acknowledged. We would also like to thank *Svenskt Limträ AB* for assisting the project by supplying all glulam beams.

References

Aicher S, Höfflin L (2004) New design model for round holes in glulam beams. Proceedings of 8th World Conference on Timber Engineering, Vol. 1, pp. 67-72, Lahti, Finland

Aicher S, Höfflin L (2006) Tragfähigkeit und Bemessung von Brettschichtholzträgern mit runden Durchbrüchen - Sicherheitsrelevante Modifikationen der Bemessungsverfahren nach Eurocode 5 und DIN 1052. Materialprüfungsanstalt (Otto-Graf-Institut), Universität Stuttgart

Aicher S, Höfflin L, Reinhardt HW (2007) Runde Durchbrüche in Biegeträgern aus Brettschichtholz. Teil 2: Tragfähigkeit und Bemessung. Bautechnik 84, Heft 12, pp. 867-880

Aicher S, Schmidt J, Brunhold S (1995) Design of timber beams with holes by means of fracture mechanics. CIB-W18/28-19-4, Copenhagen, Denmark

Carling O (2001) Limträhandbok. Svenskt Limträ AB, Print & Media Center i Sundsvall AB

Danielsson H (2007) The strength of glulam beams with holes - A survey of tests and calculation methods. Report TVSM-3068, Division of Structural Mechanics, Lund University

Danielsson H (2008) Strength tests of glulam beams with quadratic holes – Test report. Report TVSM-7153, Division of Structural Mechanics, Lund University

Danielsson H (2009) The strength of glulam beams with holes - A probabilistic fracture mechanics method and experimental tests. Report TVSM-3069, Division of Structural Mechanics, Lund University

Danielsson H, Gustafsson PJ (2008) Strength of glulam beams with holes - Tests of quadratic holes and literature test result compilation. CIB-W18/41-12-4, St Andrews, Canada

DIN 1052:2004-08 (2004) Design of timber structures — General rules and rules for buildings

DIN 1052:2008-12 (2008) Design of timber structures — General rules and rules for buildings

EN 1995-1-1 (2004) Eurocode 5: Design of timber structures – Part 1-1: General – Common rules and rules for buildings.

Foschi RO, Folz BR, Yao FZ (1989) Reliability-based design of wood structures. Structural Research Series, Report no 34, Department of Civil Engineering, University of British Columbia

Gustafsson PJ, Enquist B (1988) Träbalks hållfasthet vid rätvinklig urtagning. Report TVSM-7042, Division of Structural Mechanics, Lund University

Gustafsson PJ, Serrano E (1999) Fracture mechanics in timber engineering - Some methods and applications. Proceedings of 1st RILEM Symposium on Timber Engineering, Stockholm, pp. 141-150

Gustafsson PJ (2002) Mean stress approach and initial crack approach. In Aicher S, Gustafsson PJ (ed), Haller P, Petersson H; Fracture mechanics models for strength analysis of timber beams with a hole or a notch - A report of RILEM TC-133. Report TVSM-7134, Division of Structural Mechanics, Lund University

Gustafsson PJ (2003) Chapter 7: Fracture perpendicular to grain - Structural applications. In Thelandersson S, Larsen HJ (ed:s); Timber Engineering. John Wiley & Sons Ltd, Chichester, pp. 103-130

Höfflin L (2005) Runde Durchbrüche in Brettschichtholzträgern - Experimentelle und theoretische Untersuchungen. PhD thesis, Schriftenreihe 90, Hrsg. Materialprüfungsanstalt (Otto-Graf-Institut), Universität Stuttgart

Norris CB (1962) Strength of orthotropic materials subjected to combined stresses. Forest Products Laboratory, Report no 1816

Riipola K (1995) Timber beams with holes: Fracture mechanics approach. J Struct Eng, 121(2):225-240

Petersson H (1995) Fracture design analysis of wooden beams with holes and notches. Finite element analysis based on energy release rate approach. CIB-W18/28-19-3, Copenhagen, Denmark

Pizio S (1991) Die Anwendung der Bruchmechanik zur Bemessung von Holzbauteilen, untersucht am durchbrochenen und am ausgeklinkten Träger. Publikation 91-1, Baustatik und Stahlbau, ETH, Zürich, Switzerland

prEN 1995-1-1 (2002) Eurocode 5: Design of timber structures – Part 1-1: General Rules – General rules and rules for buildings, Final Draft 2002-10-09

Scheer C, Haase K (2000) Durchbrüche in Brettschichtholzträgern, Teil 2: Bruchmechanische Untersuchungen. Holz Roh Werkst 58: 217-228

Schmidt J, Kaliske M (2009) Models for numerical failure analysis of wooden structures. Eng Struct 31:571-579

Sjödin J, Serrano E (2008) A numerical study of methods to predict the capacity of multiple steel-timber dowel joints. Holz Roh Werkst 66: 447-454

SS-EN 1194 (2000) Glued laminated timber – Strength classes and determination of characteristic values

Vasic S, Smith I, Landis E (2005) Finite element techniques and models for fracture mechanics. Wood Sci Technol 39:3-17

Weibull W (1939) A statistical theory of the strength of materials. Proceedings nr 151, The Royal Swedish Institute for Engineering Research, Stockholm

Figures

Tables

Table 1 Material properties used in the PFM calculations
Tabelle 1 Für PFM-Berechnungen verwendete Materialeigenschaften

Modulus of elasticity ∥	E_{xx}	13 700	MPa
Modulus of elasticity ⊥	E_{yy}	460	MPa
Shear modulus	G_{xy}	850	MPa
Poisson's ratio	ν_{xy}	0.35	-
Tensile strength ⊥	f_σ	3.0	MPa
Shear strength	f_τ	9.0	MPa
Fracture energy mode I	G_{Ic}	0.300	Nmm/mm^2
Fracture energy mode II	G_{IIc}	1.050	Nmm/mm^2
Reference volume	Ω_{ref}	31 250	mm^3
Weibull shape parameter	m	5	-

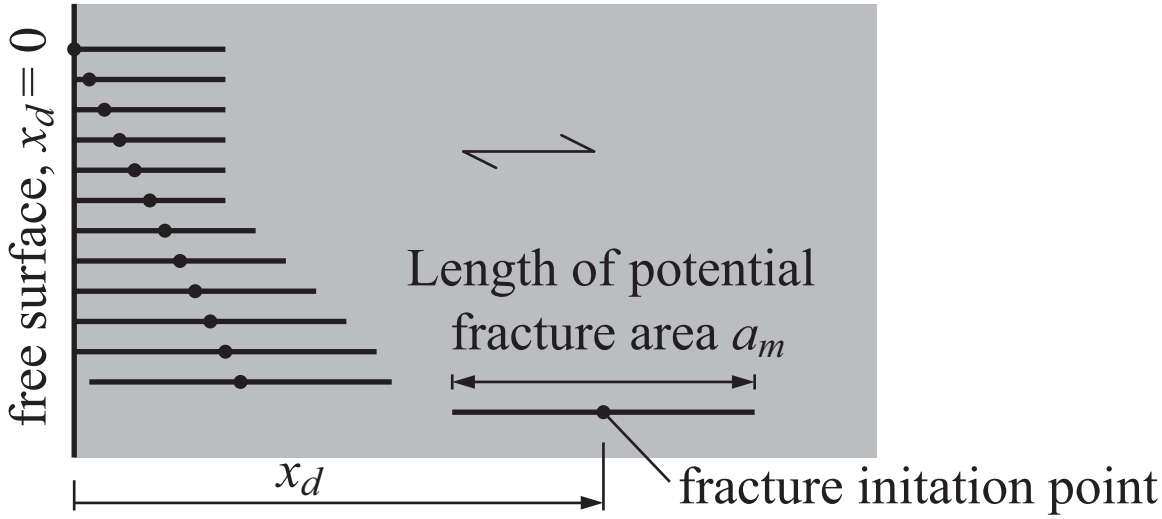
free surface, $x_d = 0$
Length of potential
fracture area a_m
x_d
fracture initation point

Fig1

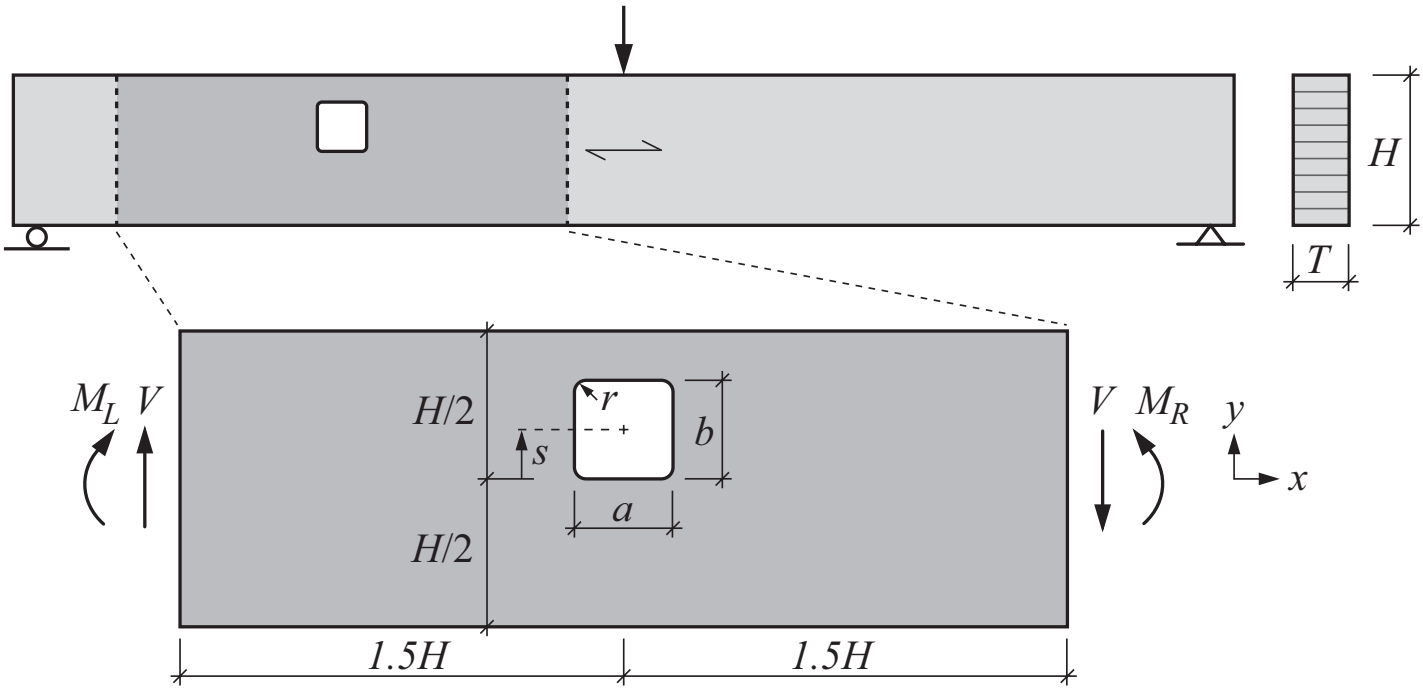

Fig2

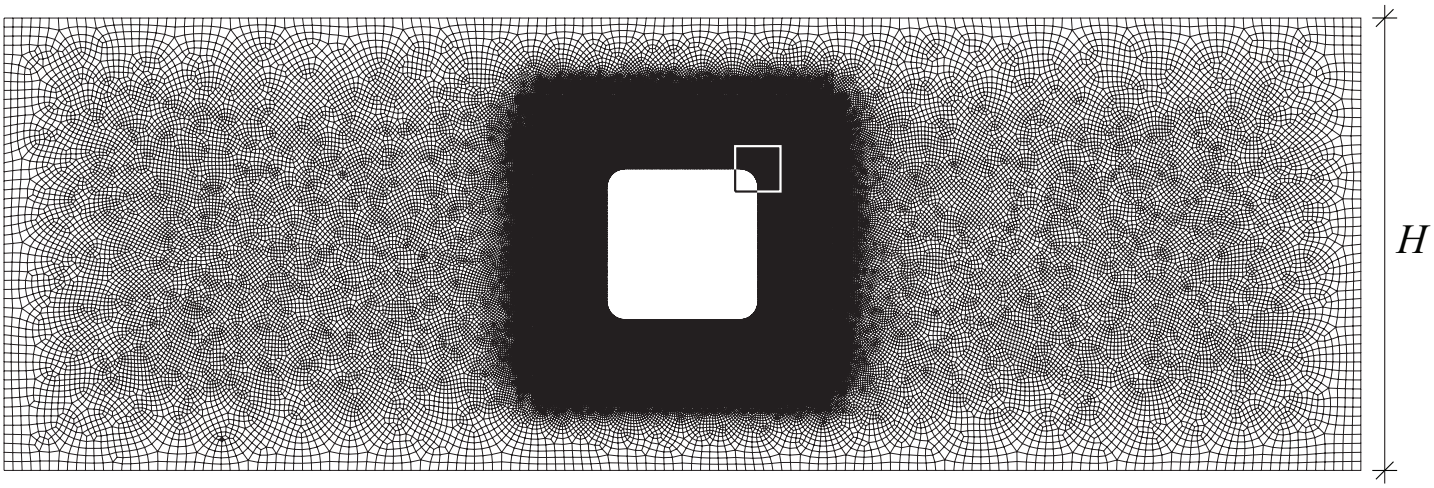

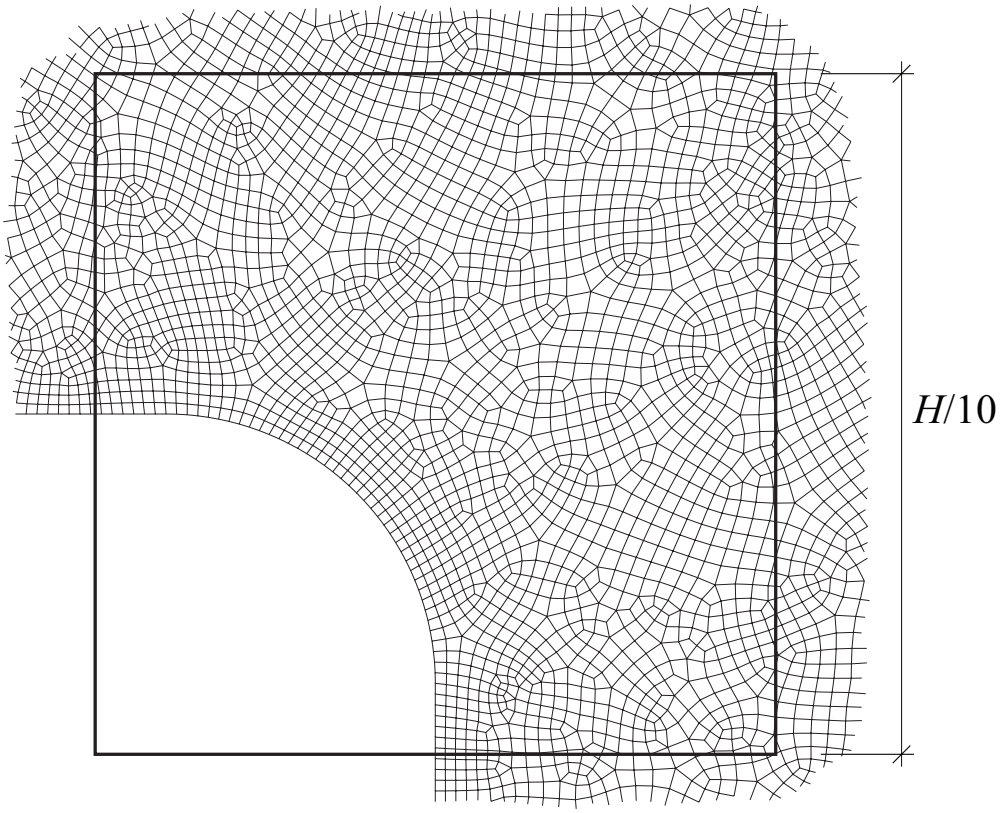

Fig3

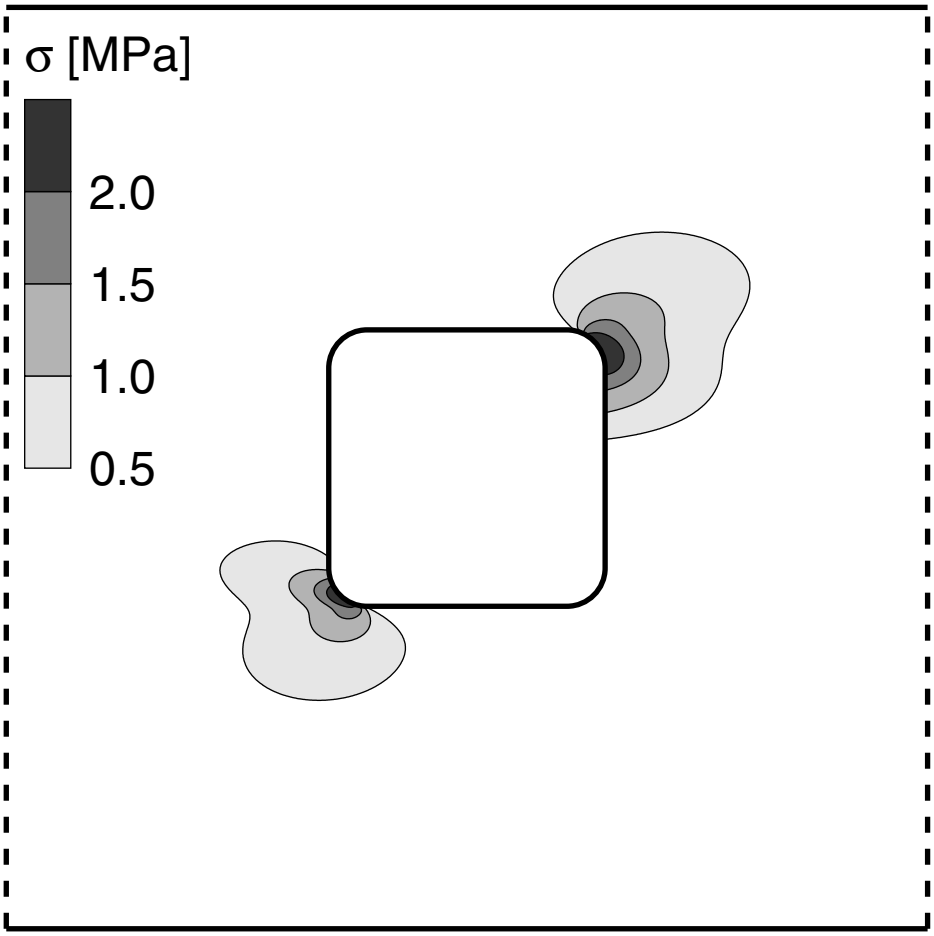

Fig4a

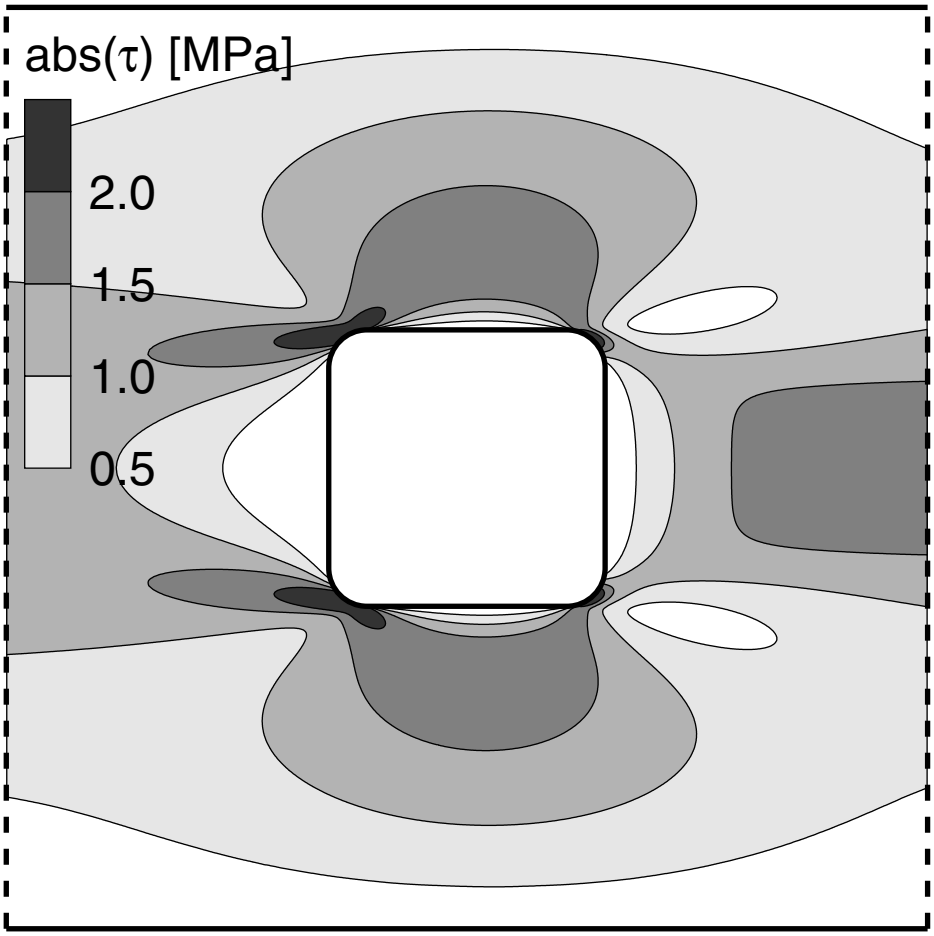

Fig4b

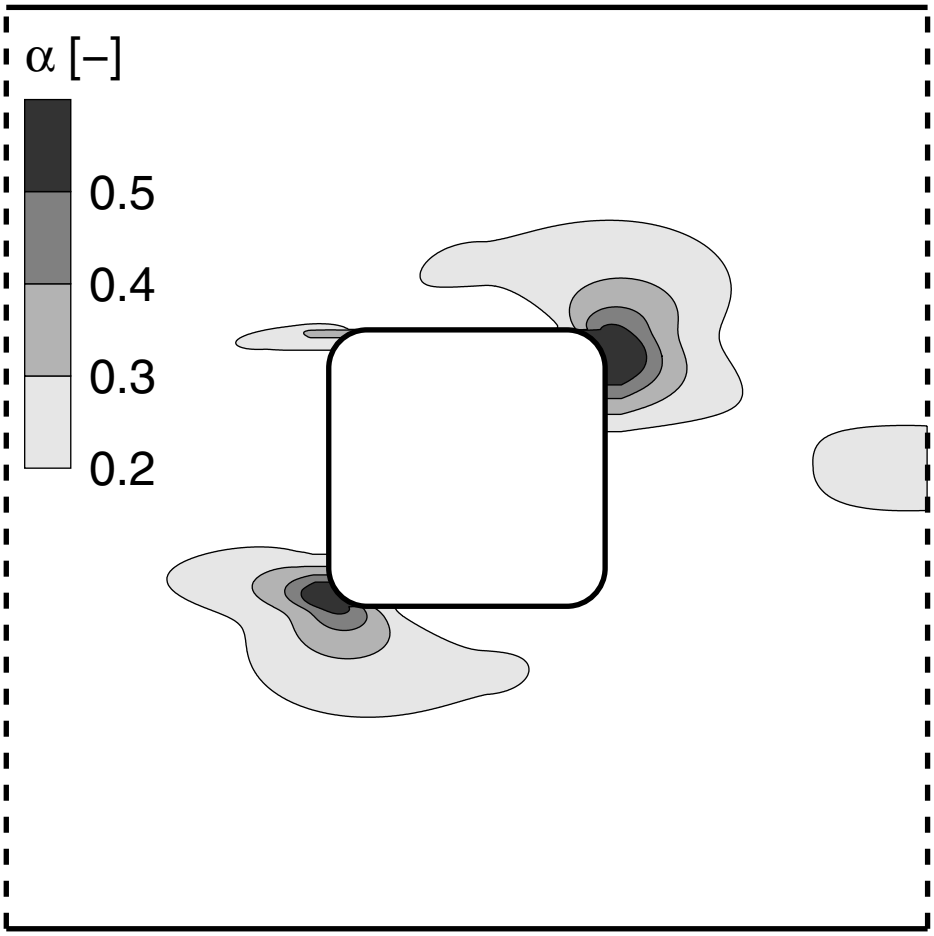

Fig4c

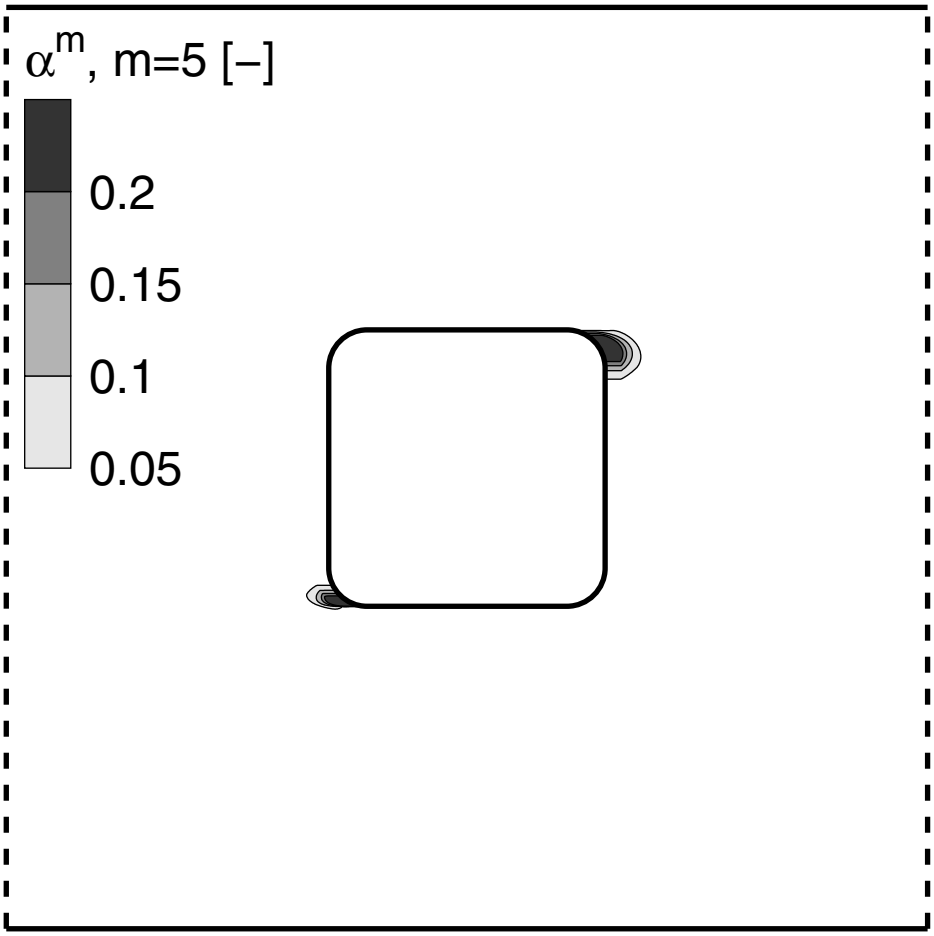

Fig4d

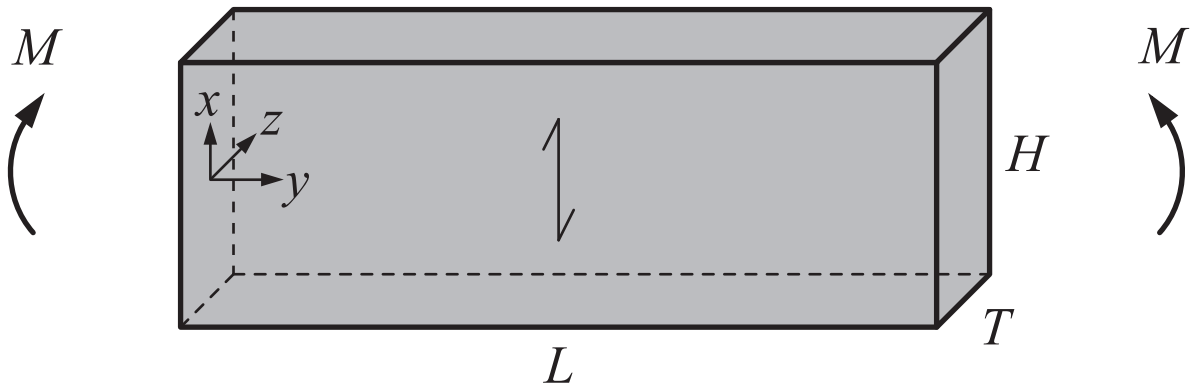

Fig5

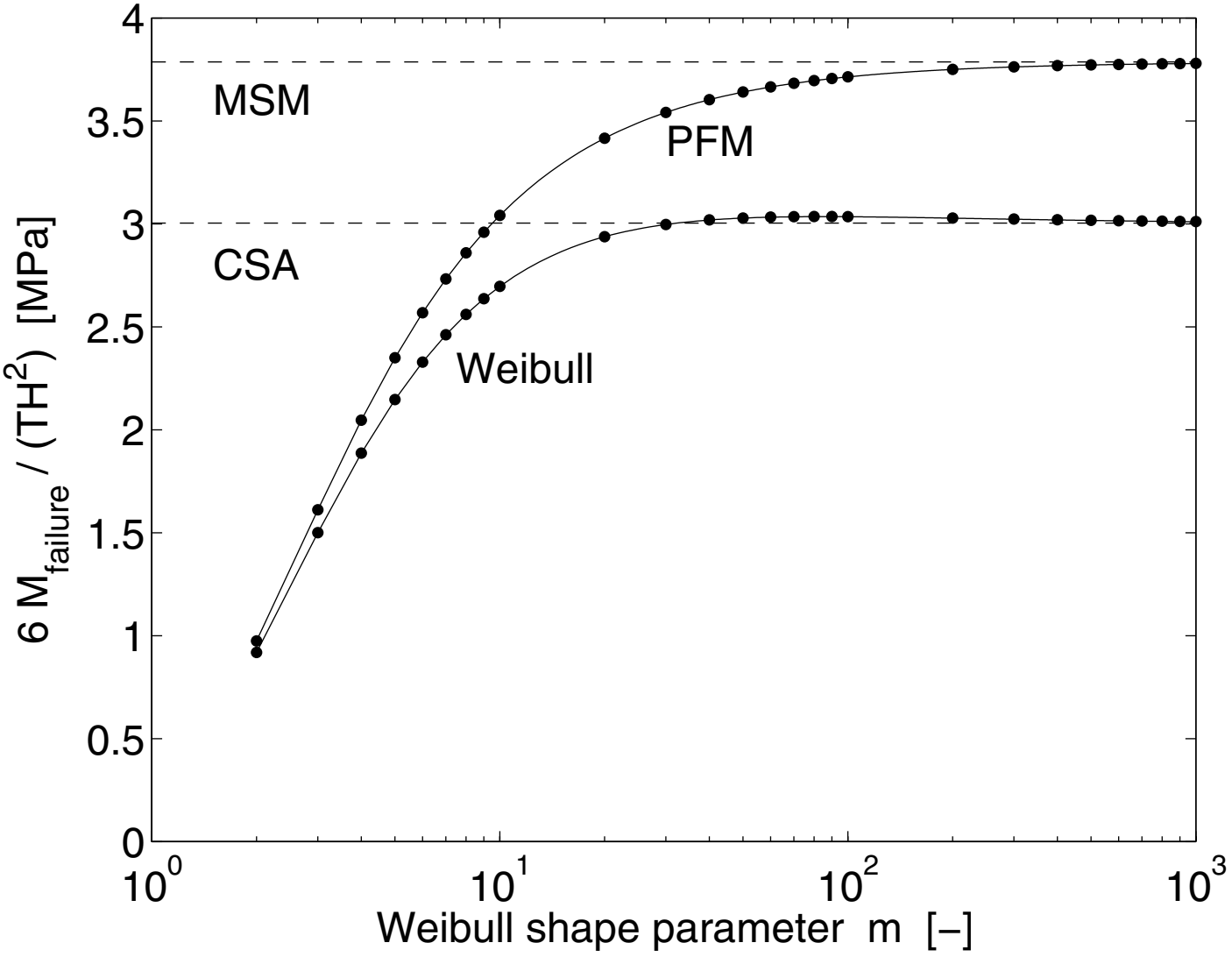
MSM
PFM
CSA
Weibull
6 M_failure / (TH^2) [MPa]
Weibull shape parameter m [–]
0
0.5
1
1.5
2
2.5
3
3.5
4
10^0
10^1
10^2
10^3

Fig6

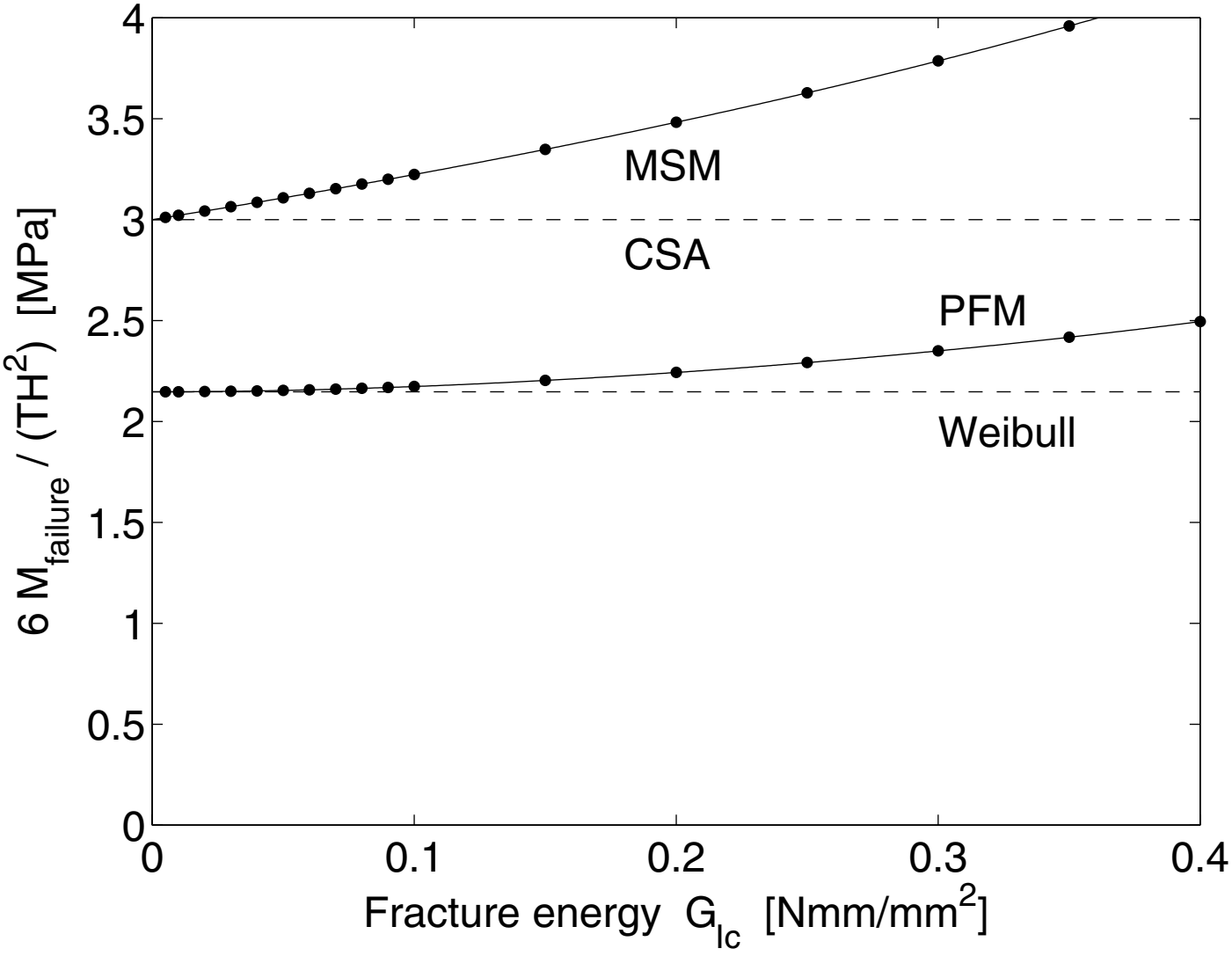
4
3.5
3
2.5
2
1.5
1
0.5
0
0
0.1
0.2
0.3
0.4
MSM
CSA
PFM
Weibull
6 M_failure / (TH^2) [MPa]
Fracture energy G_Ic [Nmm/mm^2]

Fig7

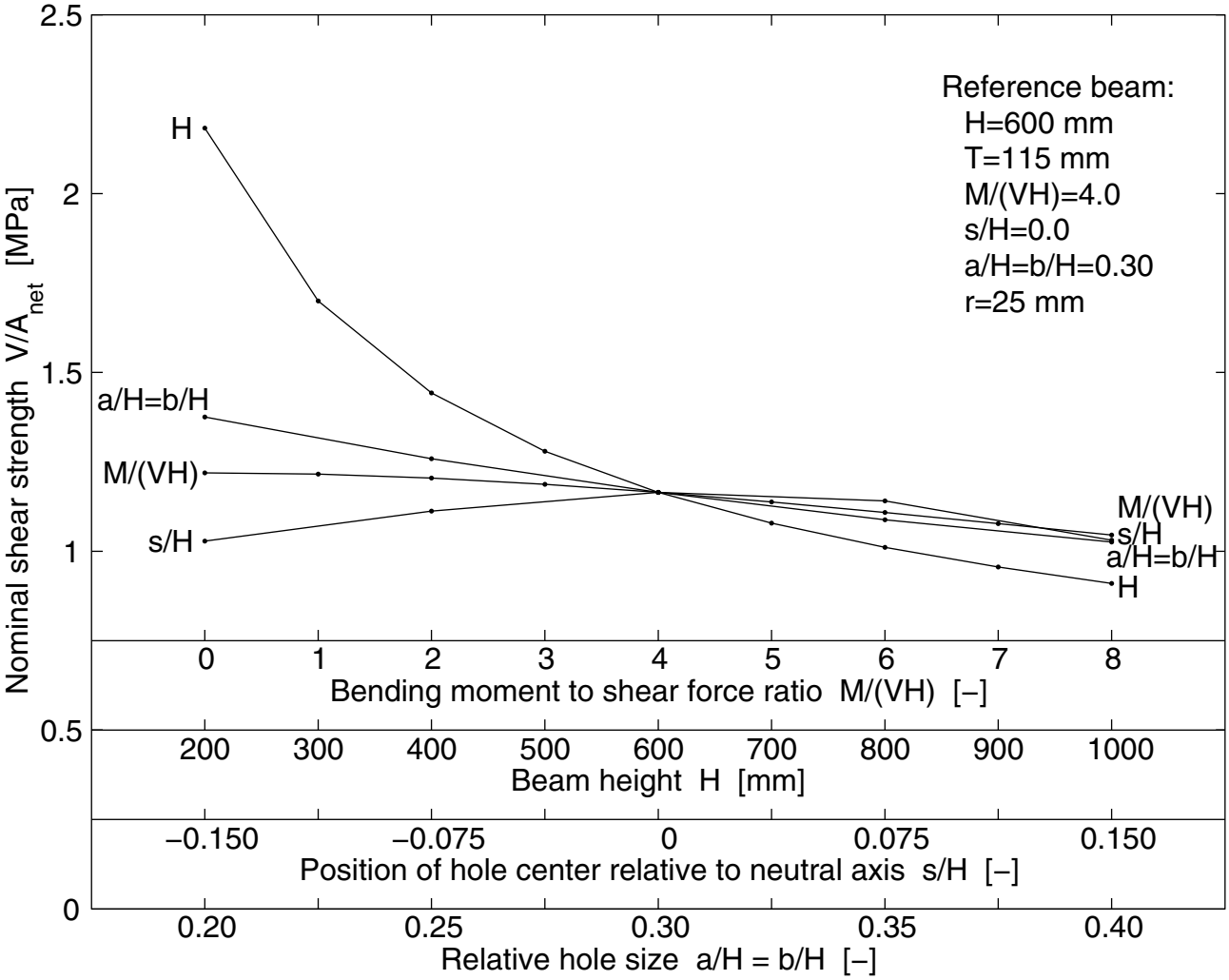
Reference beam:
H=600 mm
T=115 mm
M/(VH)=4.0
s/H=0.0
a/H=b/H=0.30
r=25 mm
H
a/H=b/H
M/(VH)
s/H
M/(VH)
s/H
a/H=b/H
H
Nominal shear strength V/A_net [MPa]
2.5
2
1.5
1
0.5
0
0 1 2 3 4 5 6 7 8
Bending moment to shear force ratio M/(VH) [–]
200 300 400 500 600 700 800 900 1000
Beam height H [mm]
–0.150 –0.075 0 0.075 0.150
Position of hole center relative to neutral axis s/H [–]
0.20 0.25 0.30 0.35 0.40
Relative hole size a/H = b/H [–]

Fig8

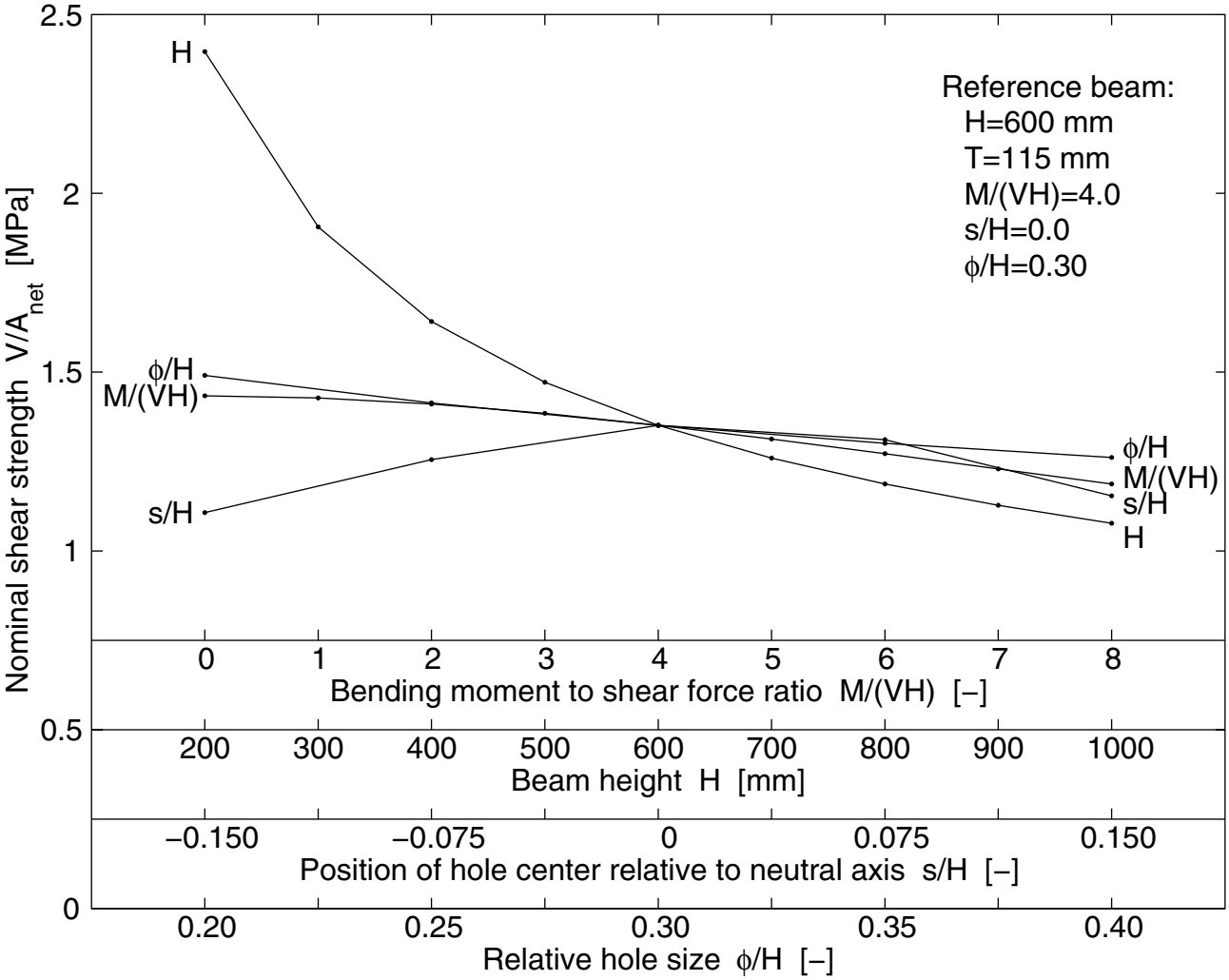
Nominal shear strength V/A_net [MPa]
2.5
2
1.5
1
0.5
0
H
φ/H
M/(VH)
s/H
Reference beam:
H=600 mm
T=115 mm
M/(VH)=4.0
s/H=0.0
φ/H=0.30
φ/H
M/(VH)
s/H
H
0 1 2 3 4 5 6 7 8
Bending moment to shear force ratio M/(VH) [–]
200 300 400 500 600 700 800 900 1000
Beam height H [mm]
–0.150 –0.075 0 0.075 0.150
Position of hole center relative to neutral axis s/H [–]
0.20 0.25 0.30 0.35 0.40
Relative hole size φ/H [–]

Fig9

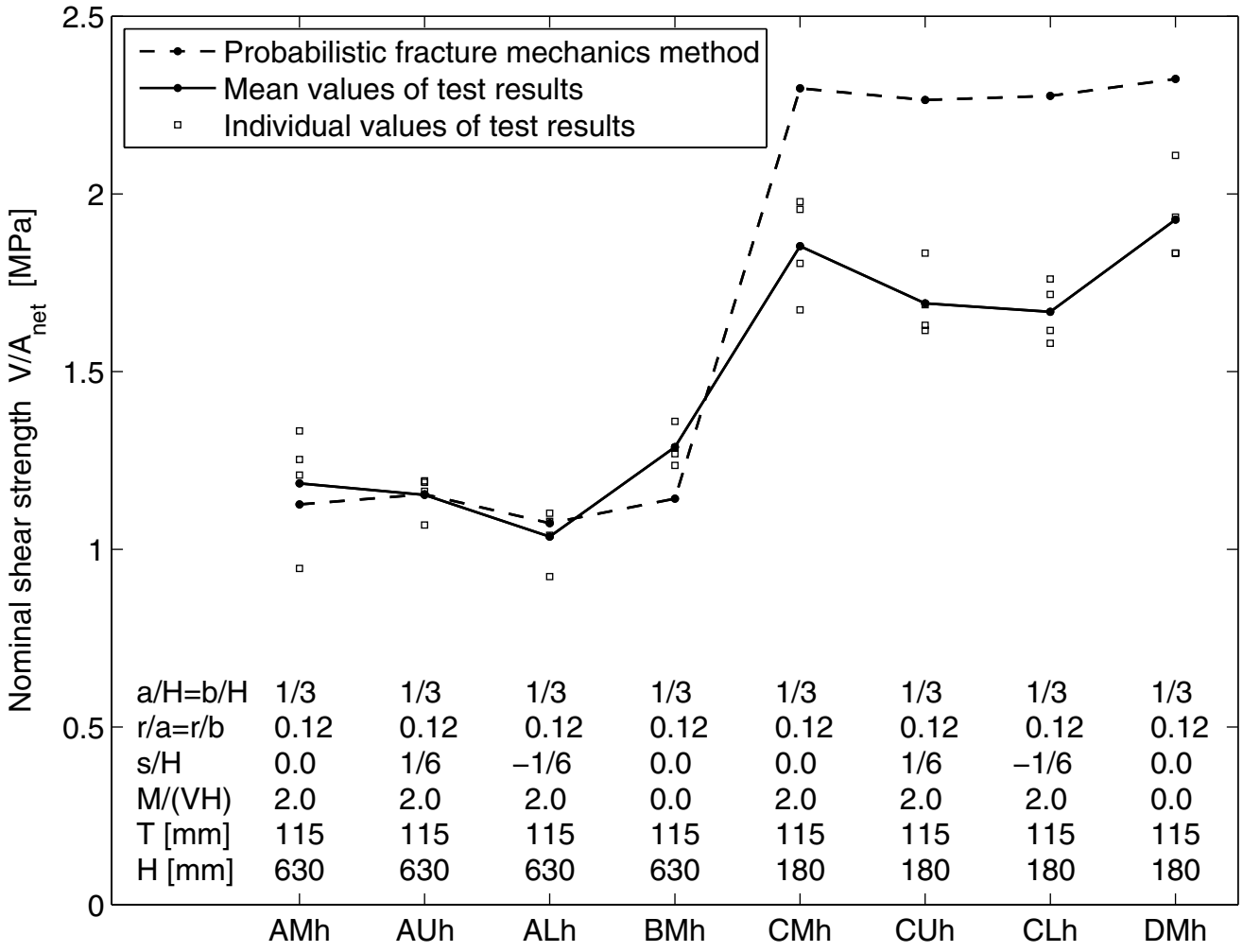
Probabilistic fracture mechanics method
Mean values of test results
Individual values of test results
Nominal shear strength V/A_net [MPa]
2.5
2
1.5
1
0.5
0
a/H=b/H 1/3 1/3 1/3 1/3 1/3 1/3 1/3 1/3
r/a=r/b 0.12 0.12 0.12 0.12 0.12 0.12 0.12 0.12
s/H 0.0 1/6 −1/6 0.0 0.0 1/6 −1/6 0.0
M/(VH) 2.0 2.0 2.0 0.0 2.0 2.0 2.0 0.0
T [mm] 115 115 115 115 115 115 115 115
H [mm] 630 630 630 630 180 180 180 180
AMh
AUh
ALh
BMh
CMh
CUh
CLh
DMh

Fig10

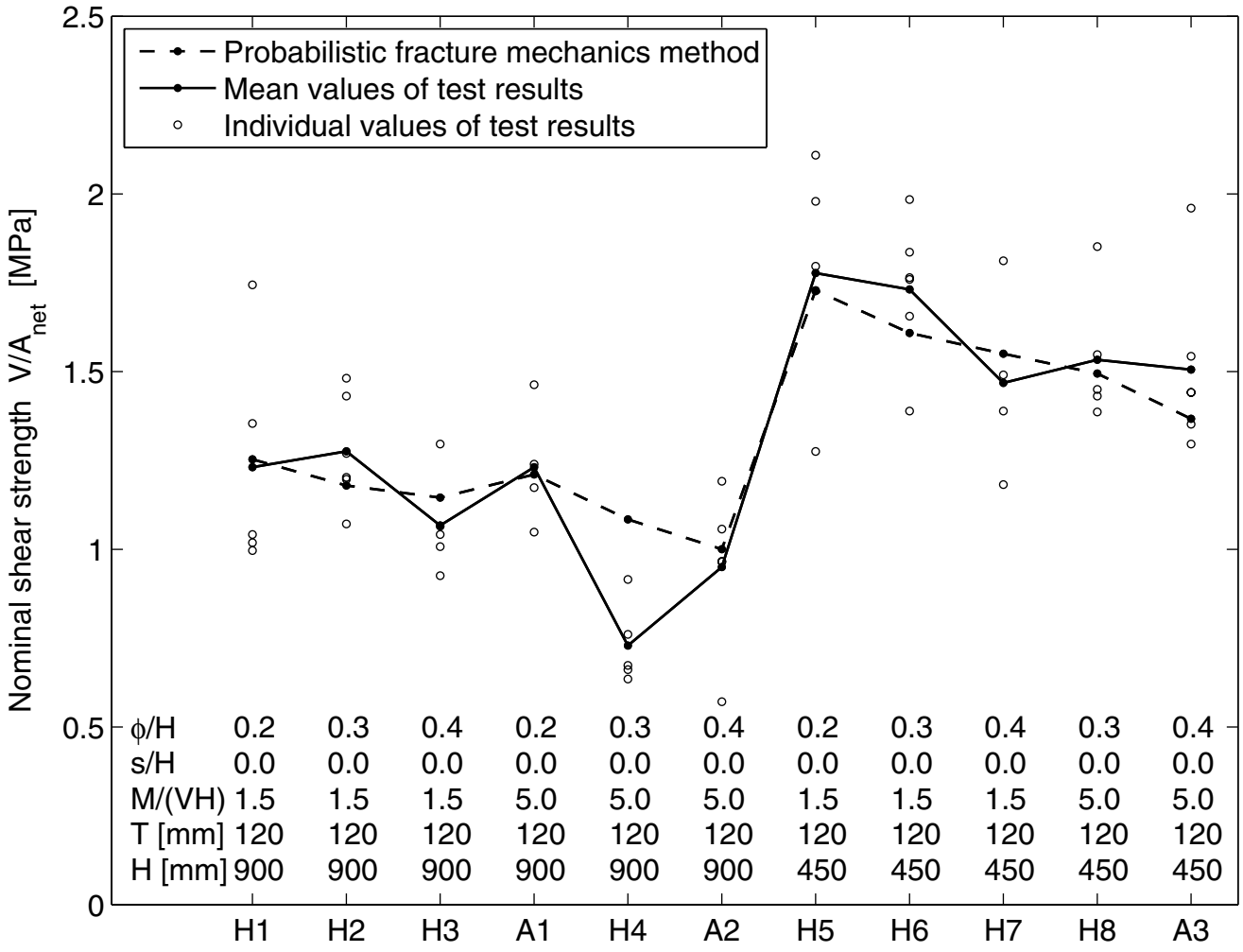
Probabilistic fracture mechanics method
Mean values of test results
Individual values of test results
Nominal shear strength V/A_net [MPa]
2.5
2
1.5
1
0.5
0
ϕ/H 0.2 0.3 0.4 0.2 0.3 0.4 0.2 0.3 0.4 0.3 0.4
s/H 0.0 0.0 0.0 0.0 0.0 0.0 0.0 0.0 0.0 0.0 0.0
M/(VH) 1.5 1.5 1.5 5.0 5.0 5.0 1.5 1.5 1.5 5.0 5.0
T [mm] 120 120 120 120 120 120 120 120 120 120 120
H [mm] 900 900 900 900 900 900 450 450 450 450 450
H1 H2 H3 A1 H4 A2 H5 H6 H7 H8 A3

Fig11

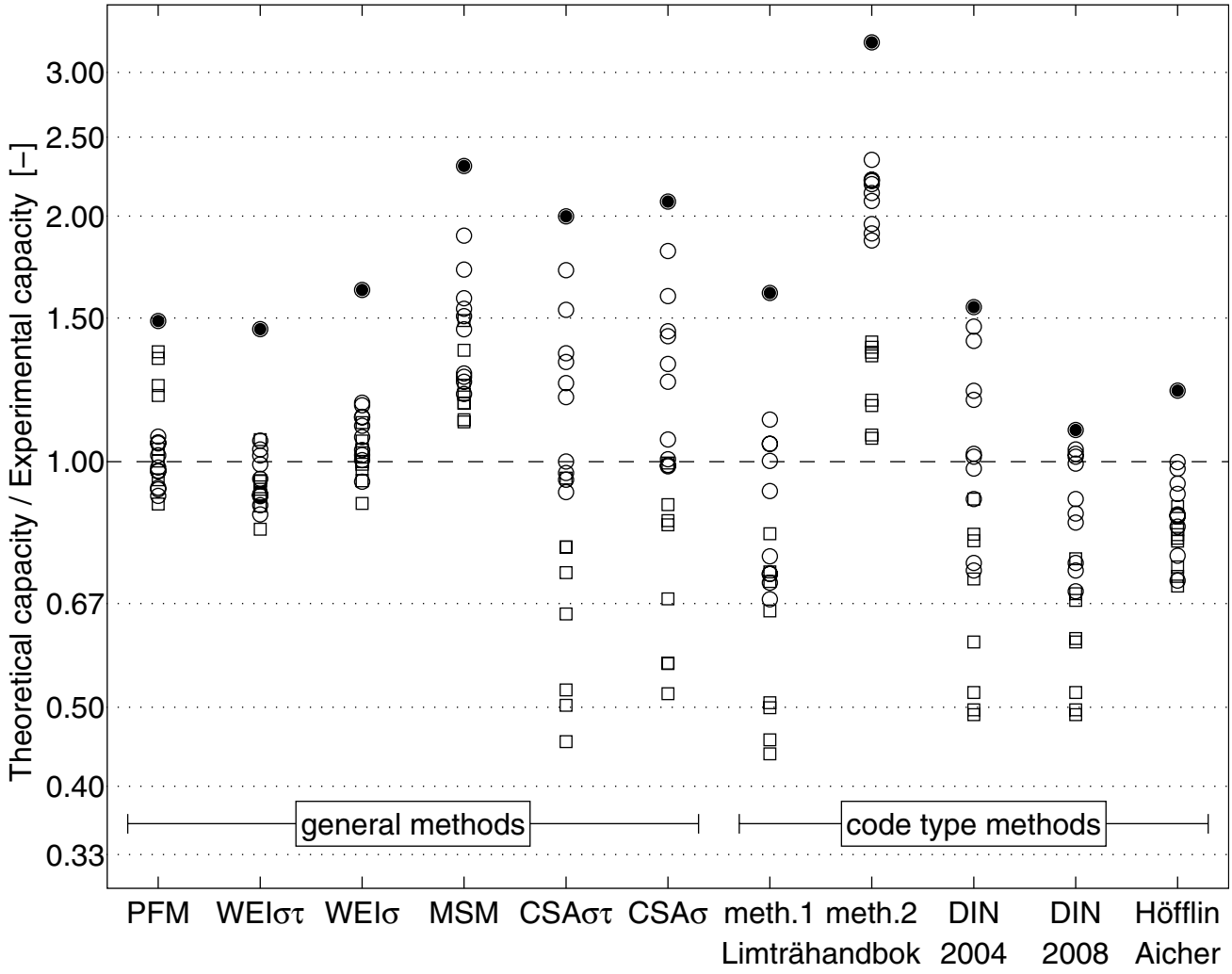
Theoretical capacity / Experimental capacity [–]
3.00
2.50
2.00
1.50
1.00
0.67
0.50
0.40
0.33
general methods
code type methods
PFM
WEIστ
WEIσ
MSM
CSAστ
CSAσ
meth.1
Limträhandbok
meth.2
DIN
2004
DIN
2008
Höfflin
Aicher

Fig12